8

Switched capacitor circuits

8.1 Introduction

Switched capacitor circuits, while making use of very well-established principles, appear to be a fairly recent development. The reason for this is the advance in very large scale CMOS integrated circuit technology. Switched capacitor circuits, as their name implies, are made up from switches, capacitors, and the operational amplifier circuits that are always needed to counteract the inevitable power losses and which also provide useful low impedance signal outputs. These switches, precision capacitors and good quality operational amplifiers can now all be made together within one large integrated circuit. The switches are CMOS transistors, which make excellent bilateral switches with very low on-resistance and very high off-impedance. The capacitors are MOS capacitors, which can be made in very accurate relative ratios of capacitance by controlling the area of metallisation. The operational amplifiers, which can now be made using only CMOS transistors [1], have excellent gain-bandwidth and power output.

Switched capacitor circuits can be conveniently divided into two classes. The first class exploits the concept of charge conservation. The second class could be called charge pumping circuits. These two classes are discussed in the next two sections.

8.2 Charge conservation

When a capacitor, C, is charged, so that it has a voltage, V, across it, the charge in the capacitor is

$$Q = CV. \tag{8.1}$$

This fundamental relationship suggests the possibility of effecting very

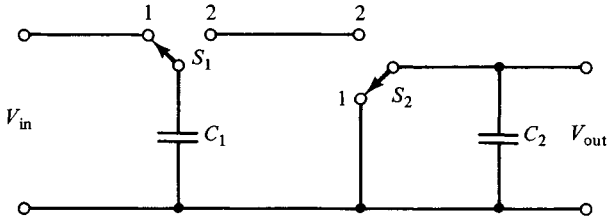

Fig. 8.1. *A switched capacitor circuit that gives voltage division.*

accurate voltage division by simply switching a charged capacitor across a second, uncharged, capacitor. The charge, Q in equation (8.1), must be conserved: it is redistributed between the two capacitors.

Fig. 8.1 illustrates this kind of circuit in its simplest form. S_1 and S_2 are break before make switches. Initially, the two switches are in position 1, so that C_1 is charged up to the voltage V_{in} and C_2 is completely discharged. The switches are then moved into position 2. Capacitors C_1 and C_2 are now in parallel and must conserve and hold the initial input charge, $C_1 V_{in}$. It follows that

$$C_1 V_{in} = (C_1 + C_2) V_{out} \tag{8.2}$$

and that the output voltage, always assuming that this is observed with an infinite impedance voltmeter, will be

$$V_{out} = V_{in} C_1/(C_1 + C_2). \tag{8.3}$$

Equation (8.3) shows that a precision voltage division may be effected by ensuring that C_1 and C_2 are made in a precision *ratio* to one another: the absolute values of C_1 and C_2 are not important. Now the value of an MOS capacitor is determined by area, and it is precisely ratios in areas that can be determined with great precision with the photolithographic process which is used in the manufacture of integrated circuits. It follows that switched capacitor circuits of the charge conservation class fit naturally into the field of VLSI CMOS circuits.

The simplest voltage division operation that can be made with the circuit shown in Fig. 8.1 is division by 2: C_1 and C_2 are made identical to one another. This binary division is central to the VLSI switched capacitor ADCs and DACs, which began to be developed in the 1970s as cheap MOS devices for digital telephony [2]. The idea of making an ADC of this kind, using discrete components, was proposed as early as 1962 by Barbour [3].

There are other kinds of ADC and DAC which may be realised using switched capacitor technique. An excellent account of these may be found in chapter 7 of the text by Allen and Sánchez-Sinencio [4], who give many

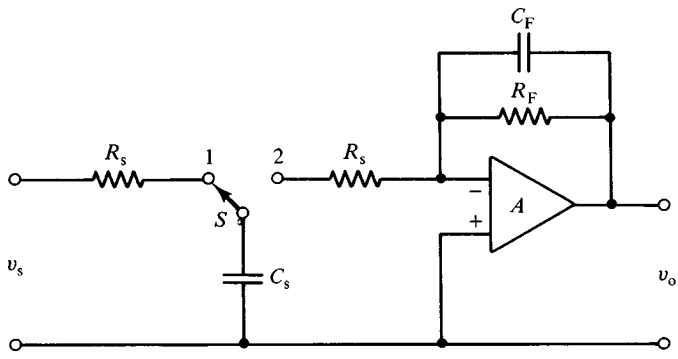

Fig. 8.2. A charge pump circuit. Switch S is break before make and is in position 1 for time $T_s/2$, and then in position 2 for time $T_s/2$, this cycle repeating every T_s.

references. These circuits will not be discussed further in this book, however, because it is not easy to propose interesting experimental circuits in this area which can be built easily. This does not imply that switched capacitor ADCs and DACs in VLSI CMOS are not important, they most certainly are, but circuits which use the switched capacitor technique in the charge pumping mode, the subject of the next section, allow a great variety of experimental work to be done. For this reason, this chapter concentrates on circuits of this charge pumping class.

8.3 Charge pumping

In the class of switched capacitor circuits that can be called charge pumping circuits, attention is directed on only one capacitor at a time in the circuit. This particular capacitor is being charged and then discharged, repetitively. It is the *frequency* of charging and discharging which is now one of the most important variables in the problem, whereas frequency was not mentioned at all in the previous section.

Fig. 8.2 shows an example of a switched capacitor circuit which operates in the charge pumping mode. C_s is charged up to the signal input voltage, v_s, when the switch, S, is in position 1. The resistance which determines how fast C_s can charge up is shown as R_s in Fig. 8.2, and represents the total circuit resistance. This is made up of the source resistance, the series resistance of the capacitor, and the resistance of the switch; the latter being by far the most important when the switch is realised by means of CMOS transistors. It is assumed that $C_s R_s$ is very small compared to the time that the switch remains in position 1. The capacitor will then be charged up to the level of the input signal voltage, v_s.

https://doi.org/10.1017/CBO9781139170246.009 Published online by Cambridge University Press

The switch is, as in the previous circuit, a break before make switch. When it is moved into position 2, shown in Fig. 8.2, capacitor C_s is completely discharged into the virtual earth of the operational amplifier, A. The current pumped into the virtual earth must then be a series of exponential pulses, having the form $(v_s/R_s)\exp(-t/C_s R_s)$, occurring every T_s, where T_s is the period of the switching frequency, f_s. The mean current flowing into the virtual earth will then be

$$\bar{\imath} = (1/T_s)\int_0^{T_s} (v_s/R_s)\exp(-t/C_s R_s)\,dt. \tag{8.4}$$

Because the assumption $C_s R_s \ll T_s$ is essential to the operation of any charge pumping circuit, the upper limit of integration in equation (8.4) may be replaced by infinity. The mean current is then given by the very simple result,

$$\bar{\imath} = C_s v_s/T_s \tag{8.5}$$

which shows up the charge pumping concept very clearly: every T_s a charge $C_s v_s$ is delivered to the virtual earth of the operational amplifier, A, in Fig. 8.2.

If the time constant $C_F R_F$, in Fig. 8.2, is made very much greater than T_s, the output of the circuit will take up a voltage level $-\bar{\imath}R_F$. The circuit shown in Fig. 8.2 may now be looked at in two different ways.

If the switching frequency, $f_s = 1/T_s$, is taken to be the input variable to the circuit, and if v_s is taken to be a constant, V_s, then Fig. 8.2 may be thought of as a precision frequency to voltage converter. This follows because the output voltage will be given, using equation (8.5), by

$$v_o = -(C_s R_F V_s)f_s. \tag{8.6}$$

This kind of voltage to frequency converter will be illustrated by the first experimental circuit of this chapter.

The second way of looking at the basic circuit shown in Fig. 8.2 is to consider the case of constant switching frequency, f_s, and then let the input signal voltage, v_s, be the variable. Always assuming that $C_F R_F \gg T_s$, the output from the circuit shown in Fig. 8.2 may then be written

$$v_o = -(R_2/R_1)\,v_s \tag{8.7}$$

where $R_2 = R_F$ and $R_1 = 1/C_s f_s$. From this point of view, the switched capacitor arrangement at the input of the operational amplifier, shown in Fig. 8.2, is behaving as though it were a 'resistor'

$$R_1 = 1/C_s f_s. \tag{8.8}$$

Equation (8.8) is a very important result because a 'resistor' which has a value determined by a capacitance, C_s, and a frequency, f_s, can be made

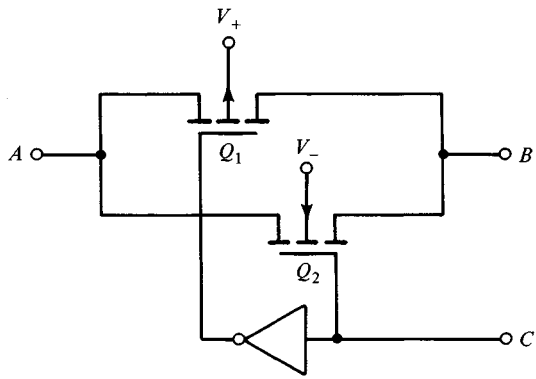

Fig. 8.3. *A CMOS bilateral switch.*

very precise and will be linear and temperature independent [5, 6]. What is even more exciting is that the value of this 'resistor' can be varied over a wide range by simply varying the switching frequency, f_s. This idea leads the circuit designer to begin proposing all kinds of switched capacitor versions of well-known analog circuits, like active filters, oscillators, phase locked loops (PLLs), and so on, which, in their conventional form, would have their performance controlled by variable resistors.

It is circuits of this kind that occupy the main area of interest in the field of switched capacitor circuits, as can be seen from the first six chapters of the text by Allen and Sánchez-Sinencio [4]. It should be mentioned that the literature, and also the background work in this field, is quite overwhelming. A very interesting review of this has been published by Weinrichter [7], who pointed out that the concept expressed here by equation (8.8) can be found in J. C. Maxwell's classical work, *Electricity and Magnetism*, which was first published in 1873.

8.4 Switch realisation

A single FET may be used as a switch, and this is the solution adopted in many switched capacitor circuits. Two problems do come up here, however. The first is the unavoidable charge injection from the gate of the transistor into the signal line which is being switched. The second problem is that performance must be influenced by the voltage level on the signal line, because this must change the gate to source voltage.

A way of getting around these two problems, while at the expense of more circuit complexity and increased parasitic capacitance, is to use a pair of CMOS transistors, as shown in Fig. 8.3. Here the p-channel enhancement MOST, Q_1, has its n-type substrate connected to V_+, and its

gate must be made negative in order to turn it fully on. The opposite applies to Q_2, the n-channel enhancement MOST. This has its p-type substrate taken to V_-, and its gate must be made positive in order to turn it fully on. The two gates can then be driven, as shown in Fig. 8.3, by simply separating them with a standard CMOS inverter. The control input, C, then accepts the standard CMOS input levels [8].

Such a CMOS bilateral switch is quite symmetric. It should be possible to balance the charge injected into the signal line from the gate of Q_2 with the charge removed by the gate of Q_1. Similarly, the voltage level on the signal line, A to B, should not affect the characteristics of the switch because changes in the gate to source voltage at Q_1 should be compensated by equal and opposite changes at Q_2.

Two switches, of the kind shown in Fig. 8.3, would be needed to realise one change-over switch. It would also be necessary to arrange the control signals to these two switches in such a way that the essential break before make property is achieved. One of the many integrated circuits that are available to solve all these problems for the experimentalist is the LTC1043 [9]. This device contains two pairs of change-over switches, together with all the drive circuits needed, and an internal oscillator. Most applications, however, call for an external drive, and the LTC1043 can accept input frequencies up to a few MHz.

Armed with this valuable device, which also has an excellent application note to go with it [10], it is possible to look at a number of experimental circuits in the switched capacitor field. The first of these is a practical realisation of the basic charge pumping circuit, first shown in Fig. 8.2, when this is used as a frequency to voltage converter.

8.5 An experimental frequency to voltage converter

Fig. 8.4 shows the first experimental circuit for this chapter. The LTC1043 has a ± 4.7 V power supply to pins 4 and 17, set up by means of the two Zener diodes which are powered from the ± 15 V supply to the whole circuit. The OP07 is powered directly from the ± 15 V lines, to pins 7 and 4, not shown in Fig. 8.4, and these pins should be decoupled to ground in the usual way.

The clock input to the LTC1043 is taken to pin 16 through an 8.2 kΩ resistor. This makes it possible to drive the circuit from a simple laboratory square wave generator. The 8.2 kΩ resistor simply protects the LTC1043 against overdrive.

Only one half of the LTC1043 is used in this experimental circuit. In one position of the pair of switches, C_2 is charged up with the top of C_s

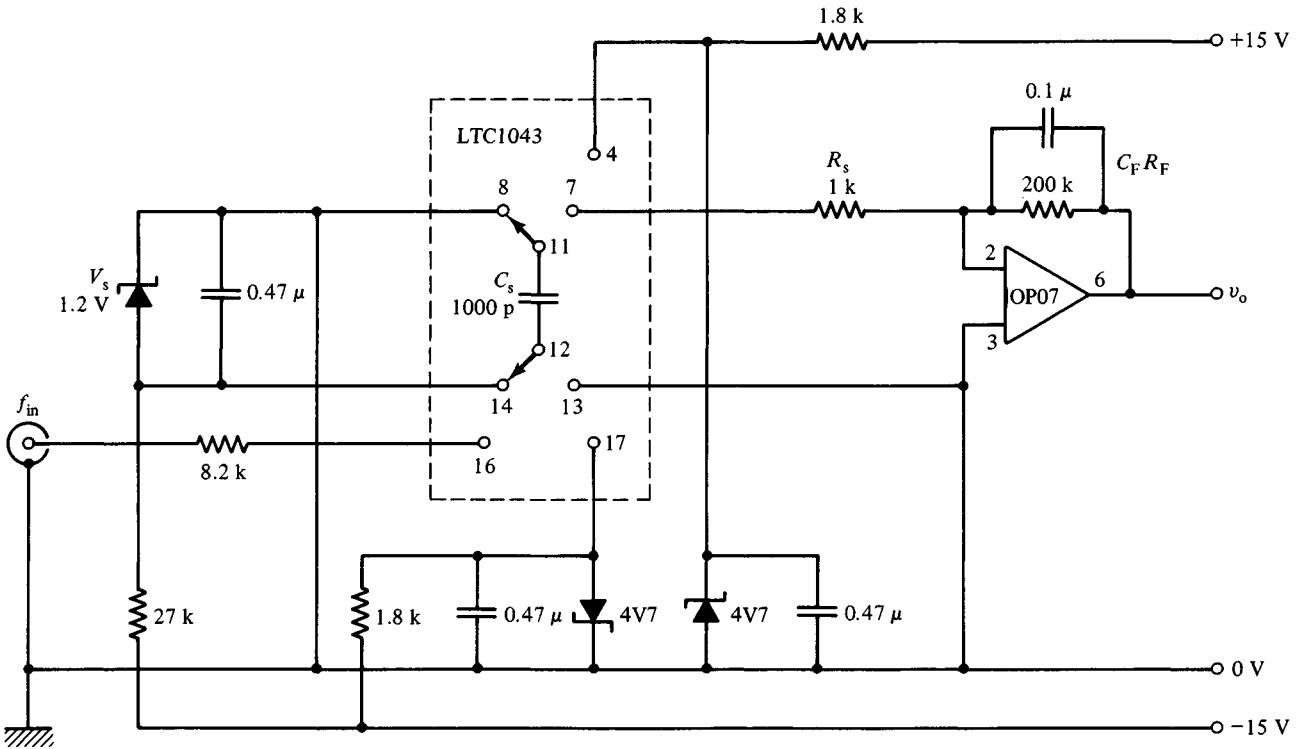

Fig. 8.4. The charge pump is used as an experimental frequency to voltage converter.

grounded and the bottom taken to -1.2 V. This -1.2 V comes from a voltage reference of the so-called bandgap variety [11]. In the second switch position, C_s is discharged into the virtual earth of the OP07, through R_s, but now the bottom of C_s is grounded and the top of C_s is connected to R_s. This illustrates the way in which two change-over switches may be used to invert a voltage in switched capacitor technique. The output from the experimental circuit, v_o, will be negative, although V_s is negative and the OP07 is being used as an inverting amplifier.

Note that pin 13 on the LTC1043 has been chosen as a grounded pin because this will disenable the charge balancing circuitry provided in the device. This is not needed in this simple application.

The values shown in Fig. 8.4 make $C_F R_F = 20$ ms. This allows the circuit to give a reasonably smooth output voltage when f_{in} is taken down as low as 500 Hz. Using equation (8.6), and substituting values for C_s, V_s and R_F, it is clear that the conversion constant of the experimental frequency to voltage converter should be 0.24 V/kHz. This means that the OP07 output voltage will limit when f_{in} is greater than 50 kHz. The linearity of the experimental circuit should be checked over this frequency range: 500 Hz–50 kHz.

So far the experimental circuit has been considered in the steady state: f_{in} is constant and v_o is constant. Even when this is true, the circuit's dynamics must be considered because of the sampled data nature which is intrinsic to any switched capacitor circuit. Considerations along these lines bring up the reason for including R_s in the circuit. Surely the circuit would work better with $R_s = 0$ so that C_s could discharge as rapidly as possible?

Looking at pin 2 of the OP07 with a sensitive wide-band oscilloscope will show the function of R_s clearly. If R_s is short circuited, the virtual earth of the OP07 will be seen to rise by some 600 mV, as C_s discharges, and this considerable overload of the OP07 input will be seen to persist for some 3 μs. When R_s is made 1 kΩ again, the input overload is completely over in 1.5 μs. Viewing pin 7 on the LTC1043 will show a smooth exponential decay from about 700 mV with a time constant of 1.5 μs. This shows that, with C_s at 1000 pF, the total resistance in series with C_s, as it discharges into the virtual earth, is around 1.5 kΩ. With $R_s = 1$ kΩ, this implies that each switch contributes 250 Ω. This agrees with the data given for the LTC1043.

The experimentalist should also look at the effect of replacing the OP07 with a faster precision operational amplifier, like the OP15, LF356 or OP27. The input overload is almost unobservable with these fast amplifiers, always provided that $R_s = 1$ kΩ is still in circuit.

The transfer function, $F(s)$, of the frequency to voltage converter shown in Fig. 8.4 may be obtained by considering the currents flowing into the virtual earth of the OP07. These must sum to zero, so that

$$C_s V_s f_{in} + v_o/R_F + C_F \, dv_o/dt = 0. \tag{8.9}$$

Writing $\tilde{f}_{in}(s)$ as the Laplace transform of the varying input frequency, $f_{in}(t)$, and $\tilde{v}_o(s)$ as the Laplace transform of the output voltage, $v_o(t)$, it follows from equation (8.9) that

$$F(s) = \tilde{v}_o/\tilde{f}_{in} = -C_s R_F V_s/(1 + sC_F R_F) \tag{8.10}$$

and this transfer function will be used later in this chapter when the circuit shown in Fig. 8.4 is used again as part of another experimental circuit.

Finally, the ripple on the output of the experimental circuit shown in Fig. 8.4 should be looked at carefully. Provided $f_{in} \gg 1/C_F R_F$, this ripple should be a saw-tooth waveform, and should have *constant* peak to peak amplitude of about 12 mV, for the values of C_s, V_s and C_F given in Fig. 8.4, regardless of the value of f_{in}. It is easy to show that the peak to peak amplitude of the ripple is given by $V_s(C_s/C_F)$. It is independent of the value of R_F. Increasing R_F will, of course, increase the mean output level of the circuit shown in Fig. 8.4, for a given input frequency, and so decrease the percentage ripple on the output. Such an increase in R_F reduces the maximum input frequency that the circuit can handle. The best way to increase the useful input frequency range is to increase C_F, but this slows down the response of the circuit to changes in f_{in}. Considerations of this kind come up in the next section.

8.6 An experimental voltage to frequency converter

The frequency to voltage converter that was put forward as an experimental circuit in the previous section had remarkable linearity. The conversion constant, under steady state conditions, given by equation (8.10) as $-C_s R_F V_s$ V/Hz, depends upon three well-defined circuit values, and really linear behaviour should be observed for input frequencies well above $1/2\pi C_F R_F$, right up to the input frequency which causes limiting at the OP07 output.

This linear behaviour is in great contrast to the non-linear characteristic of an earlier experimental circuit described in this book: the triangle waveform generator of chapter 7 which had the voltage to frequency characteristic shown in Fig. 7.4. This observation brings up the possibility of linearising the non-linearity of a voltage to frequency converter, by connecting a very linear frequency to voltage converter across it as a feedback network.

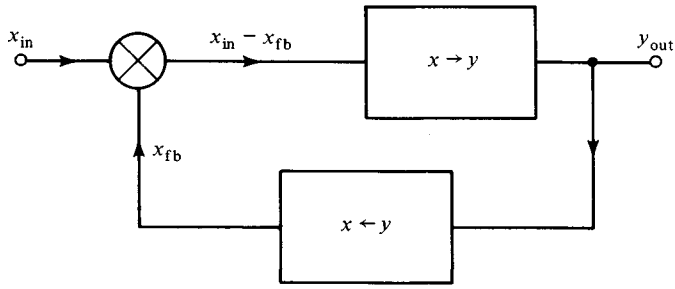

Fig. 8.5. The general feedback system where input, x, and output, y, may have different dimensions.

It should be mentioned at this point that the above idea is just one aspect of a very general idea. This is illustrated in Fig. 8.5 by the general feedback system shown there. In Fig. 8.5 an input variable, x_{in}, which could be a voltage, pressure, frequency, or any physical variable, is transformed into an output variable, y_{out}. The dimensions of x and y may be the same, as they are in the familiar feedback voltage amplifier problem, or they may be quite different: voltage and frequency, for example. The essential points in Fig. 8.5 are the feedback and the fact that the $x \rightarrow y$ function block has very high gain. The $y \rightarrow x$ feedback block is the part that determines the overall system behaviour. If the gain of the $x \rightarrow y$ function block is very high, $x_{in} - x_{fb}$ must be negligible so that x_{fb} must equal x_{in}. It then follows that y_{out} is forced to follow x_{in} with the same relationship that the feedback block, $y \rightarrow x$, sets between its input and output. The feedback system shown in Fig. 8.5 has a transfer function which is the *inverse* of the transfer function of its feedback network.

The difficulty of applying this important general principle in practice is the stability of the feedback system. This is a familiar fact to all workers in electronic circuits because of the problem of stability in connection with operational amplifiers, which are always used with feedback. In the operational amplifier case, x and y are both voltages and the feedback is done with a simple linear potential divider.

Fig. 8.6 shows how the feedback idea can be applied in the case of voltage to frequency conversion. Comparing Figs. 8.5 and 8.6, the input variables, x_{in} and v_{in}, are now both voltages and the output variables, y_{out} and f_{out}, both frequencies. The very high gain, and the differential function, both called for by the path x_{in} to y_{out} in Fig. 8.5, are realised in Fig. 8.6 by means of a simple integrator: the OP07 operational amplifier

https://doi.org/10.1017/CBO9781139170246.009 Published online by Cambridge University Press

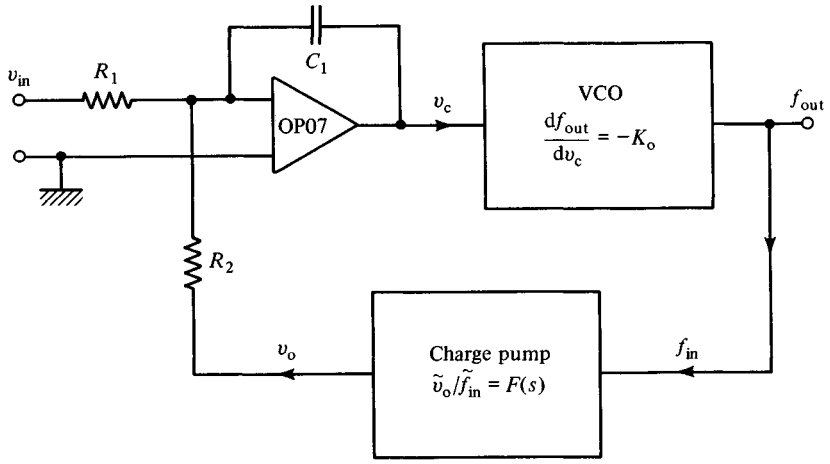

Fig. 8.6. An experimental ultra-linear VCO can be built as a control loop using the VCO of Fig. 7.2, the charge pump of Fig. 8.5 and one simple integrator.

with its feedback components, R_1, R_2 and C_1. At the virtual earth of the OP07,

$$v_{in}/R_1 + v_o/R_2 + C_1\,dv_c/dt = 0 \tag{8.11}$$

must hold.

The output frequency, in Fig. 8.6, is related to v_c by the non-linear relationship shown earlier in Fig. 7.4. In the steady state it is clear that this non-linearity will vanish from the problem because v_c is constant and equation (8.11) is simply

$$v_o = -v_{in}(R_2/R_1). \tag{8.12}$$

Now, again in the steady state, equation (8.10) reduces to

$$f_{in} = -v_o/C_s R_F V_s \tag{8.13}$$

and, of course, in Fig. 8.6 the f_{in} of the charge pump circuit, previously Fig. 8.4, is the f_{out} of the VCO, previously Fig. 7.2. Combining equations (8.12) and (8.13) thus gives

$$f_{out} = v_{in} R_2/C_s R_1 R_F V_s \tag{8.14}$$

as the characteristic of the ultra-linear VCO which should be realised by this new experimental circuit, when it is working under steady state conditions.

8.7 Stability problems

Some more theoretical work must be done before the experimental circuit shown in Fig. 8.6 can be built. This concerns its stability and is not simple because Fig. 8.6 shows a non-linear control system: it involves the VCO

which has the non-linear voltage to frequency characteristic shown in Fig. 7.4. This characteristic has a slope, using the symbolism of Fig. 8.6,

$$df_{out}/dv_c = -K_o \tag{8.15}$$

where K_o is very nearly constant, at about 5 kHz/V, over the range 2–20 kHz. At least the *change* in output frequency, for this VCO, depends fairly linearly upon a *change* in input control voltage, v_c. It follows that equation (8.15) may be used to write

$$\tilde{v}_c = -\tilde{f}_{out}/K_o. \tag{8.16}$$

Equations (8.11), (8.10) and (8.16), again writing $f_{in} = f_{out}$, then combine to give

$$\frac{\tilde{f}_{out}}{\tilde{v}_{in}} = \frac{R_2}{C_s R_1 R_F V_s}\left(\frac{1+sT_F}{1+sT_D+s^2/\omega_N^2}\right) \tag{8.17}$$

as the transfer function of the system shown in Fig. 8.6, where the filter time constant

$$T_F = C_F R_F \tag{8.18}$$

the damping time constant,

$$T_D = C_1 R_2/C_s K_o R_F V_s \tag{8.19}$$

and the natural resonant frequency,

$$\omega_N^2 = (C_s K_o V_s)/(C_1 C_F R_2) \tag{8.20}$$

all need to be chosen to optimise the system's dynamic performance. A well-designed system will show a rapid response to changes in input control voltage, with only a small overshoot. The response should not be oscillatory on the one hand nor overdamped on the other.

8.8 Measurements on the voltage to frequency converter

The value of $C_F R_F$ that was used in the first experimental circuit of this chapter, Fig. 8.4, was 20 ms. Now that Fig. 8.4 is part of the second experimental circuit, Fig. 8.6, it is sensible to leave $C_F R_F$ at 20 ms and make the system's damping time constant, T_D, also about 20 ms. With the values that have been chosen already (C_s = 1000 pF, K_o = 5 kHz/V, R_F = 200 kΩ and V_s = 1.2 V) the value of $C_s K_o R_F V_s$, in equation (8.19), is 1.2, and is dimensionless. So, if T_D is to be about 20 ms, a sensible choice for $C_1 R_2$, in equation (8.19) will also be 20 ms: for example, C_1 = 0.1 μF and R_2 = 200 kΩ. R_1 is made equal to R_2 so that $v_{in} = -v_o$ in the steady state. Note that v_{in} will thus be positive in this experiment.

https://doi.org/10.1017/CBO9781139170246.009 Published online by Cambridge University Press

This choice of values puts the natural resonant frequency of the system (equation (8.20)) close to 9 Hz, and the system should be stable.

Using the values given above, the first thing that should be measured on this new experimental circuit is its steady-state performance as a voltage controlled oscillator. In contrast to the non-linear voltage–frequency characteristic shown in Fig. 7.4, for the VCO of Fig. 7.2, the new system should have a very linear characteristic over the range 500 Hz–20 kHz. The upper frequency limit is the limit of the original VCO, as shown by Fig. 7.4, while the lower limit is where the ripple on the output of the charge pump, discussed at the end of section 8.5, begins to be significant. The voltage–frequency characteristic of this new system should extrapolate back to pass exactly through the origin, again in contrast to Fig. 7.4.

The low frequency limit can be reduced by increasing the time constants T_F and T_D, with an unavoidable reduction in system bandwidth. The bandwidth of this system is, of course, its ability to follow changes in v_{in} and reflect these changes accurately in the way that f_{out} changes. This aspect of system performance is easily measured by using a square wave generator, which has an offset facility, as an input signal. The component values being used at present make the slope of the voltage–frequency characteristic, $R_2/C_s R_1 R_F V_s$, equal to 4.17 kHz/V. An offset of +2 V on the square wave generator source will thus take f_{out} close to the centre of its range. A low level square wave on top of this +2 V, a few hundred millivolts in amplitude, for example, will then allow the dynamic system response to be seen if v_c, in Fig. 8.6, is viewed with an oscilloscope. The frequency of the square wave input must be low: about 1 Hz. A damped response should be observed, with a small overshoot, and with a response time of about 100 ms.

Another way of observing the dynamic performance is to observe the output from the system, f_{out}, when v_{in} is a low amplitude square wave at 1 Hz, added to an offset of a few volts. The oscilloscope should now be run on a much faster timebase, so that the real change in f_{out} can be seen. The output waveform will be seen to change frequency in quite a complex way, each time v_{in} changes level. A more subjective way of appreciating this complex behaviour is actually to listen to the output of the system. This is easily done by connecting a low impedance loudspeaker to the output through a 2 kΩ resistor.

The main conclusion to be drawn is that the precision voltage to frequency performance which has been obtained here has been bought at the cost of speed of response. The VCO which has been used at the heart of this experimental system was the first experimental circuit of chapter 7:

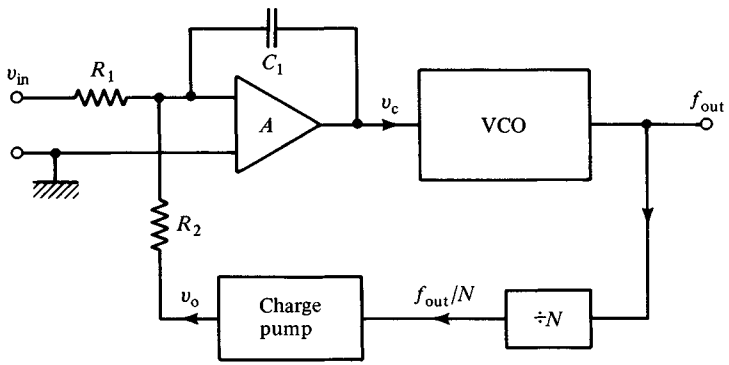

Fig. 8.7. Inserting a divider into the loop allows ultra-linear control of very high frequency voltage controlled oscillators.

the voltage controlled triangle waveform generator of Fig. 7.2. This waveform generator could change frequency very rapidly when its input control voltage was changed. In contrast, the precision VCO of the present chapter is a closed loop control system and its dynamic performance is dominated by the high gain in its input circuit, the OP07 which is being used as an integrator, and then again by the precision frequency to voltage converter which is used as the feedback path. This converter is a switched capacitor circuit which, by its very nature as a sampled data system, must include a low pass filter: the pass band must be well below the sampling frequency.

One final point concerning control loops which make use of frequency to voltage converters is the possibility of inserting a frequency divider into the loop. This is illustrated in Fig. 8.7. The input frequency to the charge pump is now only a fraction of the VCO frequency, so that the VCO can now operate at a very high frequency, this being the system output frequency, while the charge pump circuit continues to operate in the kilohertz region. Williams [12] has shown how this idea can be used to make an ultra-linear voltage to frequency converter, operating over the 100 kHz–1.1 MHz range, with a linearity of 7 ppm, despite the fact that the VCO at the heart of the system is a crude relaxation oscillator.

8.9 Switched capacitor filters

The possibility of making electronic filters by means of the switched capacitor technique was probably first put forward by Fried [13] in 1972. A review article by Solomon [14] claims that switched capacitor is now the first choice technology for filter realisation, because of the cheapness, compactness and precision that may be obtained.

The method may be introduced by considering the simple second-order active filter shown in Fig. 8.8. This is arranged as a bandpass filter and involves three operational amplifiers with feedback networks using only resistors and capacitors [15]. The labelling of the components in Fig. 8.8 may look slightly odd. The reason is that this is the circuit which is going to be used as the prototype for the last experimental circuit of this chapter, and this will involve only two operational amplifiers, A_1 and A_2, and only five capacitors. The components labelled A and R in Fig. 8.8 will be eliminated.

From the simplest point of view, a switched capacitor filter is developed from an active filter, of the kind shown in Fig. 8.8, by the technique of replacing all the resistors, which are connected to the virtual earths of the operational amplifiers, by switched capacitors. This idea was discussed in section 8.3, after equation (8.8) had been obtained, this equation showing that a resistor, R, could be replaced by a capacitor, C_s, and a switch, operating at a frequency f_s, because of the identity between R and $1/C_s f_s$.

Fig. 8.9 illustrates this idea in a particular application. The integrator on the far right of Fig. 8.8 is now shown alongside its switched capacitor equivalent. The simple integrator in Fig. 8.9(*a*) has the transfer function, to an input signal $v_1(t) = \hat{v}_1 \exp(j\omega t)$

$$\hat{v}_2/\hat{v}_1 = -1/j\omega C_5 R_4. \tag{8.21}$$

In Fig. 8.9(*b*), the resistor R_4 is replaced by capacitor C_4 and the switch, S, which is a break before make switch changing position repetitively at frequency f_s. According to equation (8.8), this is identical to a resistor $1/C_s f_s$ so that, provided $f_s \gg \omega/2\pi$, the circuit shown in Fig. 8.9(*b*) will have a transfer function

$$\hat{v}_2/\hat{v}_1 = -C_4 f_s/j\omega C_5. \tag{8.22}$$

Note that the inverting property, the minus sign in equations (8.21) and (8.22), is maintained. This is an important point because a closed loop active filter, like the one shown in Fig. 8.8, must always have an odd number of inverting operational amplifiers in its loop to ensure negative feedback. The first amplifier, A, in Fig. 8.8 is, in fact, doing nothing but inversion.

In switched capacitor technique, inversion may be done without an extra amplifier. This has already been illustrated in the first experimental circuit of this chapter, Fig. 8.4. Fig. 8.10 illustrates the point for the particular problem which is under consideration now: the switched capacitor realisation of the filter shown in Fig. 8.8. A *non-inverting*

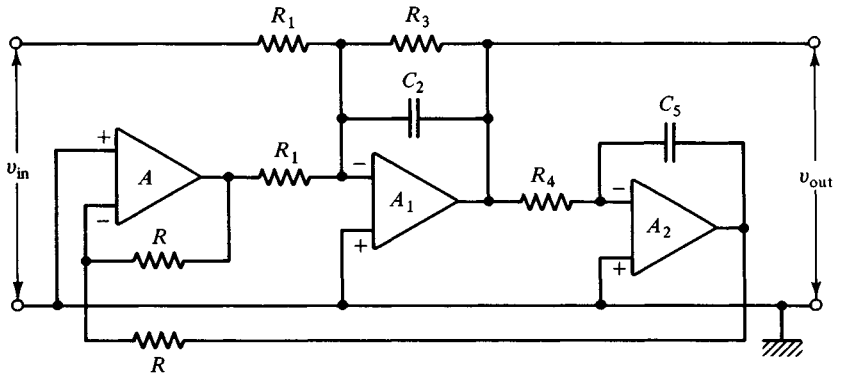

Fig. 8.8. *A bandpass active filter built using three operational amplifiers with RC feedback networks.*

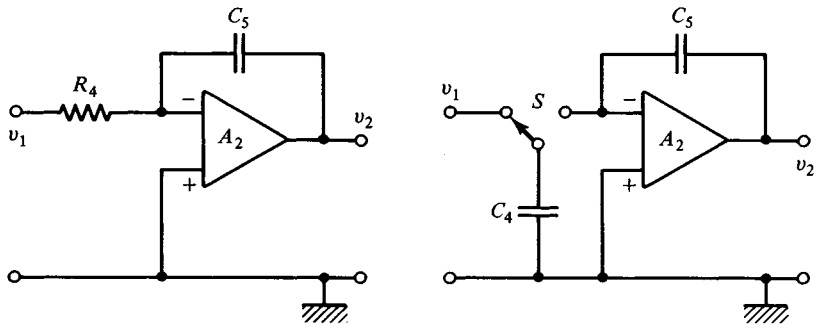

(*a*) (*b*)

Fig. 8.9. *The simple integrator* (*a*) *may be replaced by the switched capacitor circuit* (*b*) *provided the switching frequency is very much greater than the highest frequency component in the input,* $v_1(t)$.

integrator may be realised if *two* switches are used in the switched capacitor version, instead of the single switch shown in Fig. 8.9(*b*). The circuit shown in Fig. 8.10 will have a transfer function

$$\hat{v}_2/\hat{v}_1 = +C_1 f_s/\mathrm{j}\omega C_2 \tag{8.23}$$

provided $f_s \gg \omega/2\pi$. An excellent review of all these possibilities, together with the exact theory for finite switching frequency, has been given by Martin [16]. More recent work has been reviewed briefly in an important paper by Psychalinos and Haritantis [17].

Finally, the active filter circuit shown in Fig. 8.8 includes the resistor R_3 which controls the damping in this filter, and thus determines its Q. The way in which this resistor, R_3, may be replaced by a switched capacitor, C_3, is shown in Fig. 8.11.

https://doi.org/10.1017/CBO9781139170246.009 Published online by Cambridge University Press

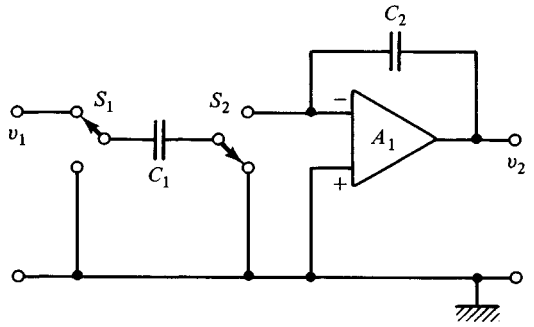

Fig. 8.10. *A non-inverting integrator in switched capacitor technique involves two break before make switches.*

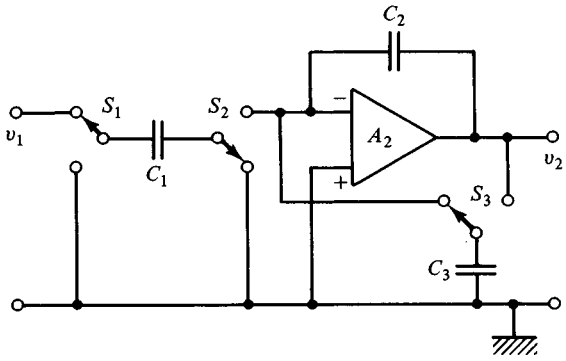

Fig. 8.11. *Damping is added to the non-inverting integrator by means of a third capacitor, C_3, and its switch, S_3.*

8.10 Filter theory

No mention has been made so far of the theory behind the active filter shown in Fig. 8.8. How are the component values for this bandpass filter to be determined? This, as throughout this book, is in the spirit of the 'circuit shape' ideas put forward in section 1.3. When a new idea in electronic circuit design comes up, it is being thought about as a sketch, a circuit shape, or circuit idea. The detailed calculation of how this idea works can only be tackled once this first stage, of sketching and arranging things, is done. This is what has been happening here in Figs. 8.9, 8.10 and 8.11.

Going back now to the simple active filter shown in Fig. 8.8, the overall transfer function of this filter is easily found by summing all the currents into the virtual earth of A_1 to zero. Assuming that the input is $\hat{v}_{in}\exp(j\omega t)$ and the output is $\hat{v}_{out}\exp(j\omega t)$, this summing may be expressed as

$$\hat{v}_{in}/R_1 + \hat{v}_{out}/j\omega C_5 R_4 R_1 + j\omega C_2 \hat{v}_{out} + \hat{v}_{out}/R_3 = 0. \qquad (8.24)$$

https://doi.org/10.1017/CBO9781139170246.009 Published online by Cambridge University Press

Equation (8.24) is considerably simplified if it is assumed that $C_2 = C_5$ and $R_1 = R_4$, in Fig. 8.8. This would be the usual choice. The natural resonant frequency of the filter is then

$$\omega_N = 1/C_2 R_1 \tag{8.25}$$

and the Q is

$$Q = R_3/R_1. \tag{8.26}$$

These expressions for ω_N and Q may then be put into equation (8.24) to give the transfer function for the filter as

$$\frac{\hat{v}_{out}}{\hat{v}_{in}} = \frac{-j\omega/\omega_N}{(1-\omega^2/\omega_N^2)+j(\omega/\omega_N Q)}. \tag{8.27}$$

The filter thus has an inverting gain of Q at its centre frequency, $\omega = \omega_N$. Its bandwidth, in hertz, is $\omega_N/2\pi Q$.

8.11 The switched capacitor version

After this theoretical digression, the method of working can go back to circuit shapes and the circuit ideas expressed in Figs. 8.9, 8.10 and 8.11. These can all be used to convert Fig. 8.8 into the switched capacitor version of one and the same bandpass filter. The result is shown in Fig. 8.12, which is the final experimental circuit for this chapter.

Fig. 8.12 shows a switched capacitor filter using two CA3140 operational amplifiers. These have the MOS input transistors which are essential for switched capacitor applications. A single LTC1043 device is used to implement the four switches which are needed. It will be clear that Fig. 8.12 is the result of combining Figs. 8.9, 8.10 and 8.11, working progressively from Fig. 8.8 to Fig. 8.12. The resistors R_1, R_3 and R_4, in Fig. 8.8, have been replaced by capacitors C_1, C_3 and C_4 in Fig. 8.12. The first amplifier, A, in Fig. 8.8 and its two resistors, both labelled R, have been replaced by the two switch arrangement, first shown in Fig. 8.10.

The natural resonant frequency of this switched capacitor filter will be given by

$$\omega_N = f_s C_1/C_2 \tag{8.28}$$

which follows from equation (8.25) when R_1 is replaced by its switched capacitor equivalent, $1/f_s C_1$. Equation (8.28) makes it immediately clear how easily a switched capacitor filter may be tuned. The switching frequency is now the variable which controls ω_N. The ratio C_1/C_2 will be constant and must, of course, be kept small so that $\omega_N/2\pi$, the frequency at which the filter is used, is always small compared to f_s. There will be

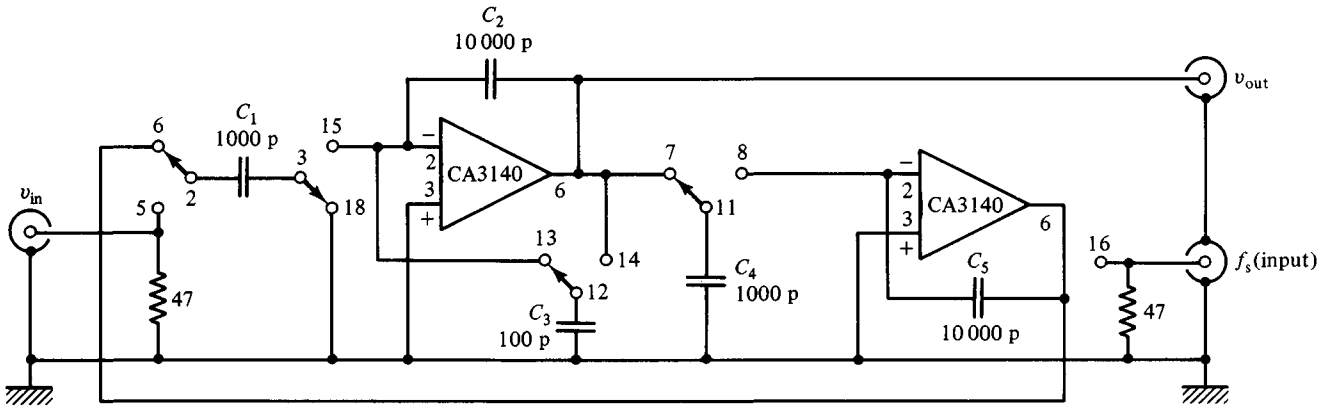

Fig. 8.12. *An experimental switched capacitor bandpass filter using two CA*3140 *operational amplifiers and one LTC*1043. *The LTC*1043 *is powered by a* ± 4.7 *V supply, as in Fig.* 8.4, *and the CA*3140*s are powered from* ± 15 *V. All devices have the usual decoupling at their power supply pins. Only the signal pins of the devices are shown here, with their numbers.*

much to say on this point when experimental work is done with the circuit shown in Fig. 8.12.

The Q of the switched capacitor filter shown in Fig. 8.12 will be given by

$$Q = C_1/C_3 \tag{8.29}$$

when the relationships $R_3 = 1/f_s C_3$ and $R_1 = 1/f_s C_1$ are substituted into equation (8.26). This shows that the Q of this switched capacitor filter does not depend upon the switching frequency, f_s. The filter may be tuned, by varying f_s, but it should always have the same Q. This constant Q property is much more difficult to obtain with the so-called biquad RC active filter, shown in Fig. 8.8, because R_3, R_1 and R_4 all need to be varied together. Usually this RC filter is tuned by changing only R_1 and R_4. This gives the filter constant bandwidth as it is tuned [15].

8.12 Construction and experimental work

The layout of the experimental circuit shown in Fig. 8.12 should be given some thought because the wiring between devices is quite complicated. Note that pin 18 on the LTC1043 has been chosen as a grounded pin, and pin 13 is taken directly to a virtual earth. This choice should disenable the charge balancing circuitry in the LTC1043 which is not needed in this application.

The level of the switching input must match the input requirements of the LTC1043. These depend upon the power supply to pins 4 and 17. When these are at ± 4.7 V, a square wave input of 5 V amplitude, that is ± 2.5 V, is ideal.

When f_s is set at 100 kHz, the values shown in Fig. 8.12 should give a filter with a sharp bandpass response at a centre frequency of 1.59 kHz. This follows from equation (8.28). The gain at this centre frequency would be expected to be 10, from equation (8.29), because C_3 is 100 pF while C_1 and C_4 are both 1000 pF. It will be found, however, that the gain is much higher than this, and a clue as to why this is so can be obtained if C_3 is increased.

Making C_3 larger, say 200 pF and then 400 pF, will reduce the gain at ω_N, and increase the bandwidth, as would be expected, but the actual value of this gain will be found to match the theoretical expectations of equation (8.29) more and more as C_3 is increased. There is clearly some intrinsic positive damping in this switched capacitor filter. In fact, making C_3 only 50 pF will make the filter unstable.

The origin of this positive damping is in the sampled data nature of the system itself. Each capacitor being switched, first accepts its charge in one

switch position, and then passes this charge on in the next half cycle of the switching input signal, f_s. This means, in the simplest case, that a time delay, $T_s/2$, is introduced by a switched capacitor input circuit. In most cases the time $T_s/2$ is quite negligible on the time scale of the signal frequency: the whole point is to use a switching frequency very much greater than the signal frequency. With a bandpass filter of the kind being considered here, however, the small time delay, $T_s/2$, represents an additional phase *lag* in the feedback loop. This lag is comparable with the small phase *advance* which C_3 introduces into the loop with the intention of obtaining high gain and narrow bandwidth at the bandpass frequency. These problems should be understood, and the first chapter of the text by Allen and Sánchez-Sinencio [4] will be valuable in this connection, as will be the review paper by Broderson, Gray and Hodges [18].

Despite the fact that the gain of the filter shown in Fig. 8.12 will be higher than expected, its performance will be found quite impressive. The centre frequency can be changed easily over the range 500 Hz–5 kHz by changing f_s. The gain at ω_N, and the filter Q, will be seen to be constant, over this entire range of tuning. The noise level at the output of the filter should be checked, when the input is short circuited. If the layout has been done well, the only noise of any importance at the output of the filter will be at f_s, and this should be only a few millivolts.

Finally, there is the interesting behaviour of the filter when an input signal close to the switching frequency, f_s, is deliberately introduced. If a signal of about 10 mV peak to peak is applied to the input of the circuit shown in Fig. 8.12, and the frequency of the input is increased, well above the value of ω_N and then still further until it equals and then exceeds f_s, a very remarkable observation will be made. As the input signal frequency passes through f_s, the output of the circuit shown in Fig. 8.12 will be a sine wave, the amplitude of this sine wave will be Q times the amplitude of the input, where Q is the gain of the filter previously measured at ω_N, but the *frequency* of this sine wave will be equal to $\omega_N/2\pi$: the bandpass frequency of the filter. This phenomenon is called *aliasing*: the process of sampling the input data, when the input data is changing at a frequency close to the sampling frequency, can reconstruct false signals at lower frequencies. A close examination of this effect, with the circuit shown in Fig. 8.12, will show that there are two input frequencies close to f_s at which an alias appears. One is $\omega_N/2\pi$ below f_s while the other is $\omega_N/2\pi$ above. This problem of aliasing is central to the field of sampled data systems: Horowitz and Hill give a brief but useful discussion in their book [19]. A detailed discussion may be found in the text by Allen and Sánchez-Sinencio [4].

8.13 Conclusions

This chapter has been dealing with just a few aspects of a new and exciting area in the field of electronic circuit design. Perhaps the most interesting feature of switched capacitor circuits is the fact that the most well-established principles, fundamental to electronic engineering, are involved. There is nothing in this chapter which Guglielmo Marconi would not have understood; in fact he would have been quite familiar with mechanically switched sampled data systems, operating up to 50 kHz, because these were used by one of his most important competitors, Rudolf Goldschmidt, before the First World War [20].

Marconi saw the future of electronics in the development of useful amplifying devices, working with continuous signals, and in this he was most certainly correct. It is interesting to reflect just how long this development has taken. Only since the mid-70s, has the electronic circuit designer been able to obtain an operational amplifier, with truly remarkable performance, as a small integrated circuit costing little more than the socket which might be used to mount it. Only in the last few years has it become possible to manufacture dozens of such high quality amplifiers, along with hundreds of other components, all together within a few square millimetres of silicon, and so realise switched capacitor filters of the advanced kind illustrated in Solomon's review paper [14].

But this is by no means the end of the story. Today, developments taking place in gallium arsenide integrated circuit processing have taken switched capacitor filter technology well up into the radio frequencies [21]. With gallium arsenide circuits, switching frequencies of several hundred megahertz are already being used, and it should be possible to enter the gigahertz area in the near future.

Notes

1 Gray, P. R., and Meyer, R. G., *Analysis and Design of Analog Integrated Circuits*, John Wiley, New York, second edition, 1984, pp. 737–64.
2 Soárez, R. E., Gray, P. R., and Hodges, D. A., *IEEE J. Sol. St. Circ.*, **SC-10**, 379–85, 1975.
3 Barbour, C. W., *Instruments and Control Systems*, **35**, No. 8, 104–5, August 1962.
4 Allen, P. E., and Sánchez-Sinencio, E., *Switched Capacitor Circuits*, Van Nostrand, New York, 1984.
5 Caves, J. T., Copeland, M. A., Rahim, C. F. and Rosenbaum, S. D., *IEEE J. Sol. St. Circ.*, **SC-12**, 592–9, 1977.
6 Hosticka, B. J., Broderson, R. W., and Gray, P. R., *IEEE J. Sol. St. Circ.*, **SC-12**, 600–8, 1977.

7 Weinrichter, H., *IEEE Circ. Syst. Mag.*, **CAS-M-6**, No. 4, 3–8, December 1984.
8 Jones, M. H., *A Practical Introduction to Electronic Circuits*, Cambridge University Press, Cambridge, second edition, 1985, pp. 227–8.
9 *1986 Linear Databook*, Linear Technology Corp., Milpitas, California, pp. 8.3–8.18.
10 Williams, J. M., Applications for a switched capacitor instrumentation building block, in: *Linear Applications Handbook*, Linear Technology Corp., Milpitas, California, 1987, pp. 3.1–3.16.
11 Easily available examples of 1.2 V bandgap voltage references devices are the Teledyne TSCO4BJ, The GE ICL8069DCZR, the Micro Power Systems MP5010GN and the Plessey ZN423T.
12 Williams, J. M., Designs for high performance voltage-to-frequency converters, in: *Linear Applications Handbook*, Linear Technology Corp., Milpitas, California, 1987, pp. 14.1–14.20. The circuit referred to is Fig. 10 of this Application Note.
13 Fried, D. L., *IEEE J. Sol. St. Circ.*, **SC-7**, 302–4, 1972.
14 Solomon, C. W., *IEEE Spectrum*, **25**, No. 6, 28–32, June 1988.
15 Horowitz, P., and Hill, W., *The Art of Electronics*, Cambridge University Press, Cambridge, second edition, 1989, pp. 276–9.
16 Martin, K., *IEEE Trans. Circ. Syst.*, **CAS-27**, 237–44, 1980.
17 Psychalinos, C., and Haritantis, I., *IEEE Trans. Circ. Syst.*, **CAS-36**, 1493–4, 1989.
18 Broderson, R. W., Gray, P. R., and Hodges, D. A., *Proc. IEEE*, **67**, 61–75, 1979.
19 Note 15 above, pp. 283 and 775–6.
20 Mayer, E. E., *Proc. IRE*, **2**, 69–108, 1914. The pages of interest are 85–92.
21 Haigh, D. G., Toumazou, C., and Betts, A. K., Switched capacitor circuits and operational amplifiers, in: D. Haigh and J. Everard (Eds.) *GaAs technology and its impact on circuits and systems*, Peter Peregrinus, London, 1989, pp. 313–56.